Journal of Coordination Chemistry
Publication details, including instructions for authors and subscription information:
http://www.tandfonline.com/loi/gcoo20

Synthesis, structure and thermokinetic studies on perchlorate salts of metal complexes containing a formamidine-type ligand

Berta Holló [a] , Vladislav Jašo [b] , Vukadin M. Leovac [a] , Vladimir Divjaković [a] , Attila Kovács [c] [d] & Katalin Mészáros Szécsényi [a]

[a] Faculty of Sciences , University of Novi Sad , Novi Sad , Serbia

[b] Faculty of Technology , University of Novi Sad , Novi Sad , Serbia

[c] European Commission, Joint Research Center , Institute for Transuranium Elements , Karlsruhe , Germany

[d] Department of Inorganic and Analytical Chemistry , Budapest University of Technology and Economics , Budapest , Hungary

To cite this article: Berta Holló , Vladislav Jašo , Vukadin M. Leovac , Vladimir Divjaković , Attila Kovács & Katalin Mészáros Szécsényi (2013) Synthesis, structure and thermokinetic studies on perchlorate salts of metal complexes containing a formamidine-type ligand, Journal of Coordination Chemistry, 66:3, 453-463, DOI: 10.1080/00958972.2012.761338

To link to this article: http://dx.doi.org/10.1080/00958972.2012.761338

Journal of Coordination Chemistry
Vol. 66, No. 3, 10 February 2013, 453–463

Taylor & Francis
Taylor & Francis Group

Synthesis, structure and thermokinetic studies on perchlorate salts of metal complexes containing a formamidine-type ligand

BERTA HOLLÓ*†, VLADISLAV JAŠO‡, VUKADIN M. LEOVAC†, VLADIMIR DIVJAKOVIĆ†, ATTILA KOVÁCS§¶ and KATALIN MÉSZÁROS SZÉCSÉNYI†

†Faculty of Sciences, University of Novi Sad, Novi Sad, Serbia
‡Faculty of Technology, University of Novi Sad, Novi Sad, Serbia
§European Commission, Joint Research Center, Institute for Transuranium Elements, Karlsruhe, Germany
¶Department of Inorganic and Analytical Chemistry, Budapest University of Technology and Economics, Budapest, Hungary

(*Received 9 July 2012; in final form 19 October 2012*)

Two formamidine-type transition metal complexes of *N,N′*-bis(4-acetyl-5-methylpyrazol-3-yl) formamidine (*ampf*) have been synthesized by a template reaction in methanolic solution of the corresponding metal perchlorates and 4-acetyl-3-amino-5-methylpyrazole (*aamp*) precursor in the presence of triethyl orthoformate. Compounds of composition $[M(ampf)(H_2O)_3](ClO_4)_2 \cdot H_2O$ ($M = Co^{II}$, Ni^{II}) have been formed. The crystal and molecular structures of the compounds have been determined by X-ray crystallography. The complexes were characterized by IR spectroscopy. The thermal stability and the decomposition kinetics of the two potential explosives were determined by thermal methods.

Keywords: Co^{II} perchlorate; Ni^{II} perchlorate; *N,N′*-Bis(4-acetyl-5-methylpyrazol-3-yl)formamidine; Thermal decomposition

1. Introduction

Pyrazole derivatives and their coordination compounds with transition metals have attracted attention due to applications in thin film precursors [1–3] or catalysts [4–6]. Many show remarkable biological activity [7–13]. Pyrazole-functionalized silica is applied for quantitative extraction and elimination of Pb^{II} from natural water [14], while trinitropyrazole derivatives were considered as potential candidates for high-energy density materials [15].

Ecologically safe "green" energetic materials have been sought [16] to replace lead azide, mercuric fulminate, *etc.* with less toxic complexes [17, 18]. Metal complexes of nitrogen-rich ligands may be suitable replacements [19, 20]. Coordination compounds

---

*Corresponding author. Email: hberta@uns.ac.rs

Journal of Coordination Chemistry
ISSN 0095-8972 print/ISSN 1029-0389 online
http://dx.doi.org/10.1080/00958972.2012.761338

mostly based on tetrazole derivatives were reported as energetic materials [21–26]. Our recent studies focused on compounds for special applications [27, 28]. Even with a negative oxygen balance, due to the relatively high nitrogen content of *N,N′*-bis(4-acetyl-5-methylpyrazol-3-yl)formamidine (*ampf*), its complexes could be candidates for high chemical energy sources. Complexes of Co^{II} and Ni^{II} with *ampf*, methanol and nitrate, synthesized recently in our laboratory [27, 28], after desolvation are relatively stable to 200 °C. Above this temperature, the decomposition takes place with a low-intensity exothermic peak even in an inert atmosphere. To examine the influence of anion on complex formation and its impact on thermal properties of potential explosives, metal perchlorate complexes with *ampf* ligand are prepared. Here, we report the synthesis, crystal structure, thermal properties, and decomposition kinetics of *ampf* complexes with perchlorate counter ion $[M(ampf)(H_2O)_3](ClO_4)_2 \cdot H_2O$ (M = Co, Ni). The assignment of the FT-IR spectra supported by density functional theory computations is attached as supporting material.

2. Experimental

2.1. *Cautions*

As perchlorates are energetic materials, special attention should be paid to protective measures during syntheses and the compounds must be handled with great care. At small-scale preparations, we encountered no difficulties.

2.2. *Materials and measurements*

All chemicals were commercial products of analytical reagent grade. IR data were collected on a Thermo Nicolet NEXUS 670 FT-IR spectrometer at room temperature using KBr disks from 4000 to 400 cm^{-1}, while in the far IR, 600–180 cm^{-1}, using CsI pellets. In all measurements, a resolution of 4 cm^{-1} was applied. Simultaneous thermogravimetry/differential scanning calorimetry data were obtained using SDT Q600 TA Instruments thermal analyzer at heating rates of 10, 5, and 2 °C min^{-1} in nitrogen (100 $cm^3 min^{-1}$) and alumina sample pan with corresponding empty reference pan. The sample mass was 0.5–0.7 mg. The molar conductivities of freshly prepared $1 \cdot 10^{-3}$ mol dm^{-3} solutions of the complexes were determined at room temperature using a digital conductivity meter Jenway 4010.

2.3. *Synthesis of the complexes*

Syntheses of the complexes were carried out by reaction of the corresponding metal perchlorates and precursor 4-acetyl-3-amino-5-methylpyrazole (*aamp*). From tested metal/ligand mole ratios, only that of 0.8/1.0 resulted in single crystal formation. The mixture of metal perchlorate and ligand precursor (0.8 and 1.0 mmol, respectively) was dissolved in 10 cm^3 MeOH by mild heating. To the warm solution, 3 cm^3 triethyl orthoformate (teof) was added continuing the heating for an additional five minutes. In 5 days, the cobalt compound precipitated in the form of orange crystals, while the nickel compound formed light blue crystals. The crystals were filtered off, washed with MeOH, and air dried. The solubility of the compounds in EtOH, MeOH, and acetone is low, but they are soluble in dimethylformamide (DMF).

[Co(*ampf*)(H_2O)$_3$](ClO_4)$_2$·H_2O (**1**), $C_{13}H_{24}N_6O_{14}Cl_2Co$: $M_r = 618.20$, yield: 30%, Λ_m(dmf) = 115 Scm^2 mol^{-1}. Selected FT-IR (KBr, cm^{-1}): 1617(vs), 1549(vs), 1416(m), 1208(m), 1145–1114(s), 1090–1040(s), 630(m), 452(m).

[Ni(*ampf*)(H_2O)$_3$](ClO_4)$_2$·H_2O (**2**), $C_{13}H_{24}N_6O_{14}Cl_2Ni$: $M_r = 617.96$, yield: 23%, Λ_m(dmf) = 121 Scm^2 mol^{-1}. Selected FT-IR (KBr, cm^{-1}): 1621(s), 1599(s), 1421(m), 1207 (m), 1146–1110(s), 1088–1036(s), 636(s), 459(m).

2.4. *Crystal structure determination and refinement*

Diffraction data were collected on an Oxford Diffraction Gemini S four-circle goniometer equipped with a Sapphire charge-coupled device detector and a graphite monochromated Mo K$_\alpha$ ($\lambda = 0.71073$ Å) X-radiation source. The crystal to detector distance was 45.0 mm. Data were reduced using the Oxford Diffraction program CrysAlis^{Pro} [29]. A semi-empirical absorption correction based on the intensities of equivalent reflections was applied, and the data were corrected for Lorentz, polarization, and background effects [30]. The structures of the complexes were solved by direct methods [31] and refined on F^2 by full-matrix least squares [32] with anisotropic temperature factors for non-H atoms. Hydrogens belonging to *ampf* were placed at calculated positions and refined with isotropic displacement parameters set to 1.2 times (1.5 for methyl) the equivalent isotropic U value of the parent atom. All hydrogens of water were found in the difference Fourier map and refined isotropic. The software used to prepare publication material included PLATON [33] and WinGX [34]. The crystallographic data and structure refinement parameters of **1** and **2** are

Table 1. Crystallographic data and structure refinement parameters for **1** and **2**.

Compound	**1**	**2**
Empirical formula	$[CoC_{13}H_{22}N_6O_5](ClO_4)_2H_2O$	$[NiC_{13}H_{22}N_6O_5](ClO_4)_2H_2O$
M_r	618.20	617.96
Crystal size	0.10 × 0.06 × 0.04	0.17 × 0.16 × 0.03
λ (Å) MoK$_\alpha$	0.71073	0.71073
Crystal system	Monoclinic	Monoclinic
Space group	P 21/c	P 21/c
a [Å]	14.9067(9)	14.8880(3)
b [Å]	13.4979(7)	13.5083(2)
c [Å]	13.1760(8)	13.0861(3)
β [°]	110.338(7)	110.295(5)
V [Å^3]	2485.8(3)	2468.39(8)
Z	4	4
D_c [g cm^{-3}]	1.652	1.663
Abs. coeff. [mm^{-1}]	0.982	1.080
F(000)	1268	1272
θ range [°]	2.96–25.00	3.13–25.00
Index ranges	$-17 \leqslant h \leqslant 17$	$-14 \leqslant h \leqslant 17$
	$-13 \leqslant k \leqslant 16$	$-16 \leqslant k \leqslant 15$
	$-15 \leqslant l \leqslant 15$	$-15 \leqslant l \leqslant 15$
Reflns. collected	11,117	12,331
Indep. reflns.	4361	4329
Parameters #	361	361
R_1	0.0523	0.0386
Gof. on F^2	1.080	1.058
Completeness	0.998	0.998

summarized in table 1. Selected metal–ligand bond distances and angles for both complexes are listed in table 2.

3. Results and discussion

3.1. *Synthesis of the complexes*

The synthesis of *aamp* [35] and its reaction with metal hydrates was already described [36, 37]. Addition of teof alters the reaction route. Teof serves as dehydrating and ligand forming agent. The methylene group of $CH(C_2H_5O)_3$ binds two *aamp* molecules and gives complexes with *N,N′*-bis(4-acetyl-5-methylpyrazol-3-yl)formamidine ligand.

Despite that teof is added in excess, during 5 days moisture from air decomposes the excess $CH(C_2H_5O)_3$, and complexes with coordinated and crystal water are formed due to the highly hygroscopic character of perchlorates. The molar conductivities of the complexes are less than that for 2 : 1 electrolytes [38] and probably refer to ion pairing or to lower mobility of the bulky complex cation in solution.

3.2. *Crystal and molecular structures of the complexes*

The molecular structures of the complexes with the corresponding atom numbering scheme are presented in figure 1. Their geometry is octahedral and slightly distorted. The *ampf* coordinates through N, N and O atoms of *ampf* ligand (in NNO mode) and forms two six-membered metallocycles with the central atom in the equatorial plane. The condensed metallocycles disturb the planarity of *ampf*. The fourth coordination place in the equatorial plane and the axial positions are occupied by waters. The asymmetric unit also comprises a lattice water. The M–L bonds are longer than 2.000 Å in both compounds; Co–ligand bonds being a bit longer than the corresponding Ni–ligand bonds are due to larger ionic

Table 2. Selected bond lengths [Å] and angles [°] for **1** and **2**.

1			
Co–O1	2.108(3)	Co–O4	2.052(3)
Co–O2	2.113(4)	Co–N1	2.087(3)
Co–O3	2.114(4)	Co–N3	2.057(3)
O4–Co–N1	91.5(1)	O2–Co–O3	83.9(2)
N1–Co–N3	87.5(1)	O3–Co–N1	96.0(1)
N3–Co–O2	87.9(1)	N3–Co–O4	175.8(1)
O4–Co–O2	93.1(1)	N1–Co–O2	175.4(1)
N1–Co–O1	93.8(1)	O1–Co–O3	167.2(1)
O1–Co–O2	87.0(1)		
2			
Ni–O1	2.084(3)	Ni–O4	2.012(2)
Ni–O2	2.076(3)	Ni–N1	2.045(2)
Ni–O3	2.091(4)	Ni–N3	2.016(2)
O4–Ni–N1	93.22(9)	O2–Ni–O3	84.6(1)
N1–Ni–N3	88.1(1)	O3–Ni–N1	95.6(1)
N3–Ni–O2	87.8(1)	N3–Ni–O4	176.34(9)
O4–Ni–O2	90.9(1)	N1–Ni–O2	175.9(1)
N1–Ni–O1	93.3(1)	O1–Ni–O3	168.4(1)
O1–Ni–O2	87.1(1)		

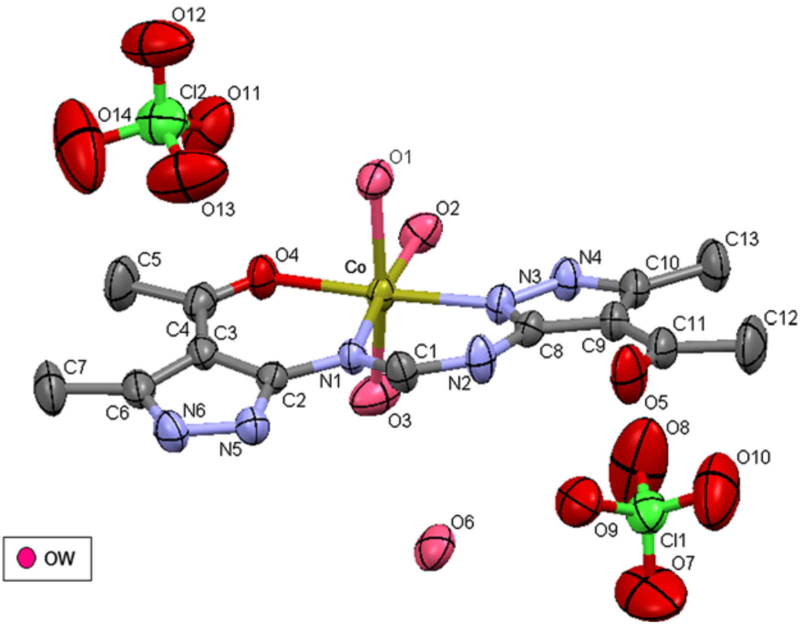

Figure 1. The molecular structure [39] of **1**. Hydrogens are omitted for clarity. The molecular structure of **2** is identical.

radius of Co^{II}. The *ampf* donors bond stronger to the metal center in both compounds than water as supported by somewhat longer $M–OH_2$ bonds. The values of angles N1–M–O1 and N1–M–O3 are larger while the O2–M–O1 and O2–M–O3 are lesser than 90° referring to a higher repulsion between *ampf* and axially positioned water than between water molecules in the equatorial and axial positions. The six-membered metallocycles (M–N1–C2–C3–C4–O4 and M–N1–C1–N2–C8–N3) deviate from planarity in both complexes. The values of the torsion angles of N1–M–N3–C8 and O4–M–N1–C2 from the two metallocycles are –10.3(3)° and 8.7(3)° in **1** and –10.7(3)° and 8.2(2)° in **2**, similar to the structures with *ampf* published earlier [27, 28]. The *trans* angles in **1** and **2** are less than 180°. On the basis of the crystallographic data, we conclude that the complexes are isomorphous and isostructural.

Beside the ionic interactions, perchlorate ions are strongly bonded to complex cations by hydrogen bonds. Perchlorate ions are bonded to all surrounding water and *ampf* molecules, generating three-dimensional (3D) hydrogen-bonded networks in the crystal. A part of 3D H-bonding between complex cations, perchlorates, and crystalline water molecules is viewed nearly along the *a* axis which is shown in figure 2. H-bonds between complex cations are responsible for formation of relatively well-separated column-like arrangement consisting of structural units arranged in layers perpendicular to the *b* axis. The layers in direction of the *a* axis form interspaces approximately positioned on (¼, ¼, *c*) and (¾, ¾, *c*). The lattice water stabilizes the structure by hydrogen bonds. The most important H-bond distances with corresponding angles are listed in table 3.

Despite nitrate and perchlorate compounds with similar composition formed, the structures of the complexes with perchlorate are significantly different. In the perchlorate compounds $[M(ampf)(H_2O)_3]^{2+}$, $M = Co^{II}$, Ni^{II}, with distorted octahedral geometry in the

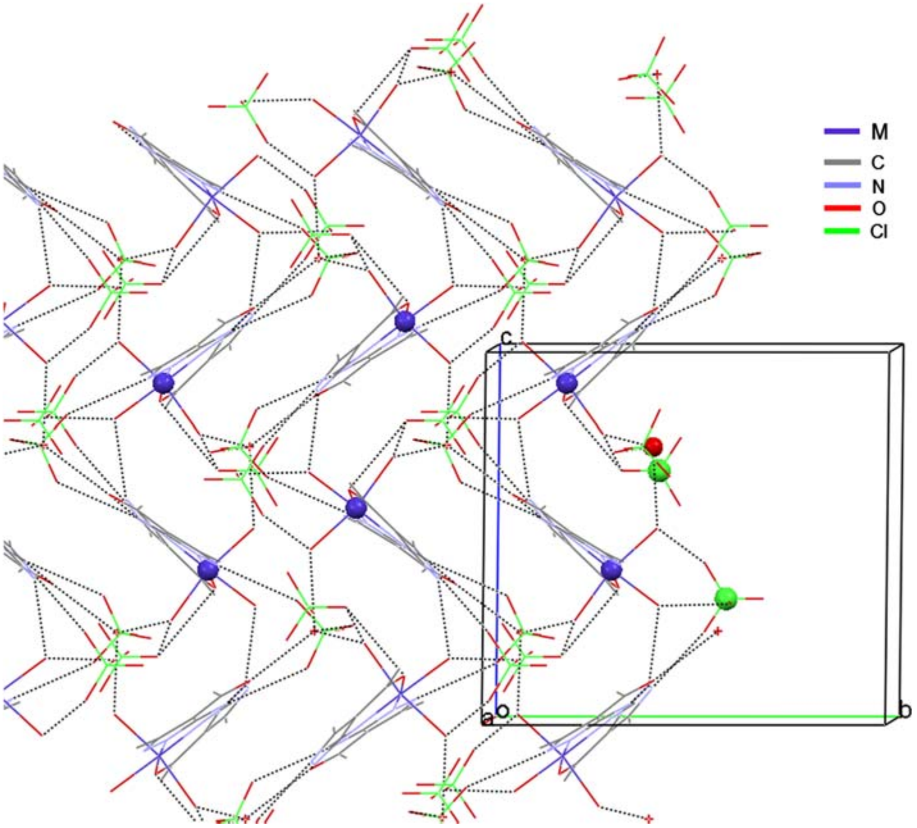

Figure 2. A part of the 3D H-bonding (dashed lines) between complex cations, perchlorates, and crystalline water viewed nearly along the *a* axis. M = Co^{II} and Ni^{II}. Hydrogens are omitted for clarity.

Table 3. H-bond distances [Å] and angles [°] in **1** and **2**.

	D. . .A [Å]		D–H. . .A [°]	
Donor–H. . .acceptor	**1**	**2**	**1**	**2**
O1–H1wa. . .O6 (*x*, ½−*y*, −½+*z*)	2.762(6)	2.758(5)	169(5)	164(4)
O1–H1wb. . .O11 (*x*, *y*, *z*)	2.912(6)	2.935(4)	157(7)	170(5)
O2–H2wa. . .N5 (*x*, ½−*y*, −½+*z*)	2.766(5)	2.776(3)	175(6)	169(5)
O2–H2wb. . .O14 (1−*x*, −½+*y*, 1.5−*z*)	2.927(7)	2.898(5)	162(7)	158(4)
O3–H3wa. . .O6 (*x*, *y*, *z*)	2.794(5)	2.806(4)	165(6)	170(5)
O3–H3wb. . .O12 (1−*x*, −½+*y*, 1.5−*z*)	2.943(7)	2.989(5)	163(8)	142(5)
O6–H6wa. . .O5(2−*x*, −½+y, 2.5−*z*)	2.810(5)	2.816(4)	173(6)	172(5)
O6–H6wb. . .O9 (*x*, *y*, *z*)	2.865(7)	2.859(5)	172(6)	150(6)
N2–H2. . .O7 (2−*x*, −½+*y*, 2.5−*z*)	2.948(6)	2.916(5)	132.1(3)	132.4(2)
N2–H2. . .O5 (*x*, *y*, *z*)	2.747(4)	2.740(3)	130.6(2)	129.8(2)
N4–H4. . .O8 (2−*x*, −*y*, 2−*z*)	2.970(7)	2.960(5)	159.1(3)	158.0(2)
N6–H6. . .O13 (1−*x*, 1−*y*, 2−*z*)	2.934(6)	2.928(5)	172.6(3)	171.0(2)

second coordination sphere is surrounded by perchlorate ions and, besides the water from the first coordination sphere, with a water of crystallization, too. As a consequence, the number of H-bonds is three times higher than corresponding nitrates. In addition, in the perchlorate compounds links between cations by H-bonds are mainly established through anions (cation–anion–cation pattern). On the contrary, in the corresponding nitrates, H-bonds link the cation centers directly.

The experimentally determined density of 1.6(1) $g\,cm^{-3}$ for both complexes agrees well with the calculated ones. The densities of **1** and **2** are higher by about 8% compared to the densities of the corresponding nitrate compounds. Packing of **1** and **2** is realized by 3D H-bond networks and the interspace becomes more dense than nitrates.

Both the different coordination mode and the higher density of perchlorate compounds suggest enhanced energy release potential. This is supported by the thermal measurements: the decomposition of the perchlorates is accompanied by a significantly higher exothermic effect compared to the corresponding nitrates [27, 28].

3.3. *Thermal data and kinetics of decomposition of 1 and 2*

Decomposition of **1** and **2** starts with endothermic water loss at room temperature. By controlled rate thermal analysis, the water content of both compounds is removed almost completely at ~ 150 °C. Some water residue, probably due to restricted diffusion, evaporates at a very slow rate (<0.02% min^{-1}) to above 200 °C when a rapid, highly exothermic decomposition begins. The thermal stability and the released energy accompanying the decomposition of the anhydrous cobalt(II) compound (**1**) is somewhat lower than that of **2**. Decomposition around 350 °C turns into slow endothermic reaction and in nitrogen it is not completed at 600 °C. Despite the sensitivity of potential explosives like **1** and **2** toward thermal decomposition, the repeated measurements show very similar decomposition patterns.

According to the higher sensitivity of the balance compared to the heat flow measurement, the kinetic calculations are based on the derivative thermogravimetry (DTG) data.

Decomposition of the solvent-free compounds consists of overlapping processes. For the best fit, three constituent peaks were extracted from the corresponding DTG signal for each complex. The result of the peak extraction at 5 °C min^{-1} is shown in figures 3 and 4. Isostructural compounds usually have very similar decomposition patterns [40, 41]. However, with sensitive equipment even slight differences in the decomposition can be detected [42]. The process with the highest peak temperature is clearly dominant in the decomposition of **2** while in **1** the process with central peak temperature is principal at all three heating rates. The mass loss data and peak maxima for separated processes are presented in table 4.

The thermal behavior of **1** and **2** is determined by the most intensive process. Therefore, nonisothermal kinetic parameters are calculated on the basis of the dominant process for both compounds, for **1** the second, while for **2** the third peak. However, a closer look to these processes shows that they actually start even before the water residue is completely removed, at a very slow rate (see figures 3 and 4). For determination of kinetic parameters, the model-free Kissinger plot [43] and the Ozawa's method [44] were used.

The calculation of kinetic parameters is based on the following equations:

$$\ln\left(\frac{\beta_i}{T_{\mathrm{pi}}^2}\right) = \ln\left(\frac{A_k R}{E_k}\right) - \left(\frac{E_k}{R}\right)\left(\frac{1}{T_{\mathrm{pi}}}\right) \tag{1}$$

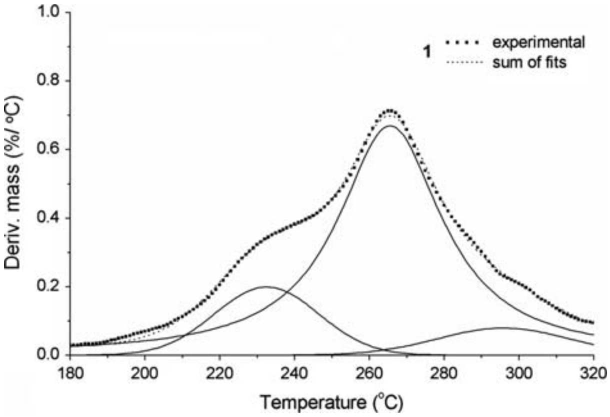

Figure 3. Extracted DTG curves for **1**.

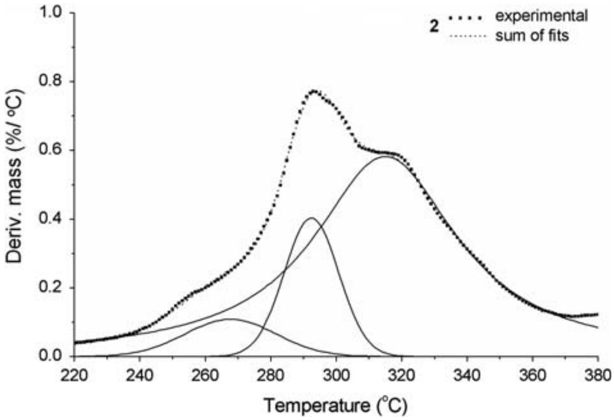

Figure 4. Extracted DTG curves for **2**.

Table 4. Mass loss data and the corresponding peak temperatures for the extracted peaks for **1** and **2** at $\beta = 2$, 5, and 10 °C min^{-1} heating rates.

β [°C min^{-1}]	Δm_1 [%]	t_1 [°C]	Δm_2 [%]	t_2 [°C]	Δm_3 [%]	t_3 [°C]
1						
2	4.3	218.0	35.9	252.1	1.3	288.3
5	6.9	232.5	35.7	265.5	3.5	295.8
10	3.7	242.9	42.2	273.6	2.1	316.0
2						
2	3.6	261.4	10.1	280.8	43.2	303.9
5	3.8	268.4	8.4	292.4	48.9	315.1
10	5.2	283.2	4.8	300.3	46.7	324.0

Table 5. Nonisothermal kinetic parameters for the dominating exothermic process for **1** and **2**.

	Kissinger's method		Ozawa's method	
	1	**2**	**1**	**2**
E_k [kJ mol^{-1}]	167.6	220.3	164.1	218.8
log(A) [s^{-1}]	14.0	17.4	11.3	12.8
r	0.996	0.999	0.997	0.999

$$\log\beta_i = \ln\left(\frac{A_oR}{E_o}\right) - \frac{0.4567E_o}{\mathrm{RT_{pi}}} \tag{2}$$

In the equations β_i denotes the heating rate, T_{pi} is the peak temperature for the corresponding heating rate, $A_{\mathrm{k}}/A_{\mathrm{o}}$ and $E_{\mathrm{k}}/E_{\mathrm{o}}$ are the pre-exponential constant and the apparent activation energy calculated by the Kissinger's/Ozawa's method, respectively. R is the gas constant. The nonisothermal kinetic parameters presented in table 5 are calculated using the data for heating rates $\beta_i = 2$, 5, and 10 °C min^{-1}. The corresponding values of A and E determined on the basis of the two methods are in good accord.

Comparison of the value of the average activation energy of 166 kJ mol^{-1} for **1** with literature data for energetic cobalt(II) complexes [19, 20] shows that the values are similar. For **2** the average value of $E_{\mathrm{a}} = 220$ kJ mol^{-1} is much higher than that found in Ni(II) 1,4-diaminobutane [45] and imidazole [46] complexes. While the strain in the metallocycles enhances the energy release [47], the measured density of 1.6(1) g cm^{-3} for **1** and **2** is common for metal complexes. The 3D hydrogen-bonded networks in the crystal stabilize the compounds at low temperatures.

4. Conclusion

Two formamidine-type complexes with perchlorate ions have been synthesized and characterized by single crystal X-ray analysis, FT-IR spectrometry, and thermal analysis. The presence of perchlorate affects the structure of the compounds. When using nitrate salts, besides an NNO coordination mode of *ampf*, one anion coordinates to the metal. In perchlorate compounds, the octahedron surrounding the metal center is established by the same coordination mode of the ligand. However, instead of perchlorate coordination, three water molecules occupy the remaining coordination sites around Co and Ni. The composition, the strain in the metallocycles and the packing of $[\mathrm{M}(\mathit{ampf})(\mathrm{H_2O})_3](\mathrm{ClO_4})_2\cdot\mathrm{H_2O}$ (M = Co, Ni) compounds refer to their enhanced energy release potential and may be regarded as high chemical energy sources. In spite of the fact that the new compounds have a somewhat lower nitrogen content (<20%) and a negative oxygen balance, their apparent activation energy falls in the range found in energetic cobalt(II) and nickel(II) complexes. Though the compounds are isomorphic and isostructural, their thermal decomposition patterns are significantly different.

Supplementary material

Crystallographic data (excluding structure factors) for **1** and **2** are deposited at the Cambridge Crystallographic Data Center under codes CCDC 865873 and CCDC 865874, respectively. These data can be obtained free of charge via http://www.ccdc.cam.ac.uk/cgi-bin/catreq.cgi. Supplementary data associated with this article can be found in the online version.

Acknowledgments

The work was financed by the Ministry of Education and Science, Republic of Serbia (Grant Nos. 172014 and III45022). V.M. Leovac and K. Mészáros Szécsényi thank Secretary for Science and Technological Development, Autonomous Province of Vojvodina, Republic of Serbia for support and KMSz also for mobility (No. 451-02011/2007-02) and the CEEPUS III Program (CIII-CZ-0212-05-1112). The authors thank Dr. Branislav Jović for recording the IR spectra.

References

[1] C. Yélamos, K.R. Gust, A.G. Baboul, M.J. Heeg, H.B. Schlegel, C.H. Winter. *Inorg. Chem.*, **40**, 6451 (2001).
[2] D. Pfeiffer, M.J. Heeg, C.H. Winter. *Inorg. Chem.*, **39**, 2377 (2000).
[3] O.M. El-Kadri, M.J. Heeg, C.H. Winter. *J. Organomet. Chem.*, **694**, 3902 (2009).
[4] P. Elo, A. Pärssinen, S. Rautiainen, M. Nieger, M. Leskelä, T. Repo. *J. Organomet. Chem.*, **695**, 11 (2010).
[5] B.A. Messerle, M.J. Page, P. Turner. *Dalton Trans*., 3927 (2006).
[6] Y. Gao, H. Li, C. Ke, L. Xie, B. Wei, Y. Yuan. *Appl. Organomet. Chem.*, **25**, 407 (2011).
[7] F.-L. Li, H.-B. Song, B. Dai, L.-F. Tang. *Appl. Organomet. Chem.*, **24**, 669 (2010).
[8] J. Fang, Z. Jin, Z. Li, W. Liu. *J. Organomet. Chem.*, **674**, 1 (2003).
[9] B. Maggio, G. Daidone, D. Raffa, S. Plescia, L. Mantione, V.M. Catena Cutuli, N.G. Mangano, A. Caruso. *Eur. J. Med. Chem.*, **36**, 737 (2001).
[10] U.N. Tripathi, G. Venubabu, M. Safi Ahmad, S.S. Rao Kolisetty, A.K. Srivastava. *Appl. Organomet. Chem.*, **20**, 669 (2006).
[11] U.N. Tripathi, M. Safi Ahmadz, G. Venubabuz, P. Ramakrishna. *J. Coord. Chem.*, **60**, 1777 (2007).
[12] N.V. Kulkarni, V.K. Revankar. *J. Coord. Chem.*, **64**, 725 (2011).
[13] J.S. Solanki, T.R. Thapak, A. Bhardwaj, U.N. Tripathi. *J. Coord. Chem.*, **64**, 369 (2011).
[14] S. Radia, S. Tighadouinia, Y. Toubia, M. Bacquet. *J. Hazard. Mater.*, **185**, 494 (2011).
[15] P. Ravi, G.M. Gore, V. Venkatesan, S.P. Tewari, A.K. Sikder. *J. Hazard. Mater.*, **183**, 859 (2010).
[16] M.B. Talawar, R. Sivabalan, T. Mukundan, H. Muthurajan, A.K. Sikder, B.R. Gandhe, A. Subhananda Rao. *J. Hazard. Mater.*, **161**, 589 (2009).
[17] A.Yu. Zhilin, M.A. Ilyushin, I.V. Tselinskii, Yu.A. Nikitina, A.S. Kozlov, I.V. Shugalei. *Russ. J. Appl. Chem.*, **78**, 188 (2005).
[18] F. Guang, Z. Yin-Li, S. Jia-Juan, Z. Min-Yan. *J. Coord. Chem.*, **64**, 3711 (2011).
[19] G.-F. Zhang, Y. Wang, M.-Y. Cai, D.-M. Dai, K. Yan, A.-S. Ma, P. Chen, R. Wang, P. Li, J.-H. Yi, F.-Q. Zhao, J.-Z. Li, X.-Z. Fan. *J. Coord. Chem.*, **63**, 1480 (2010).
[20] G. Singh, I.P.S. Kapoor, S.M. Mannan, J. Kaur. *J. Hazard. Mater.*, **A79**, 1 (2000).
[21] J. Zhang, L. Wei, Y. Cui, T. Zhang, Z. Zhou, L. Yang. *Z. Anorg. Allg. Chem.*, **637**, 1527 (2011).
[22] S. Qi, Z. Li, Z. Zhou, Y. Cui, G. Zhang, T. Zhang, J. Zhang, L. Yang. *Chin. J. Chem.*, **29**, 59 (2011).
[23] Y. Cui, T. Zhang, J. Zhang, L. Yang, J. Zhang, X. Hu. *Prop. Explos. Pyrotech.*, **33**, 437 (2008).
[24] Y. Cui, T.-L. Zhang, J.-G. Zhang, L. Yang, X.-Ch. Hua, J. Zhang. *J. Mol. Struct.*, **889**, 177 (2008).
[25] S. Wang, L. Yang, T. Zhang, G. Zhang, J. Zhang, Z. Zhou. *J. Coord. Chem.*, **64**, 2583 (2011).
[26] X.-Q. Zhang, Q. Yu, H.-D. Bian, X.-G. Bao, H. Liang. *J. Coord. Chem.*, **62**, 2108 (2009).
[27] V.M. Leovac, Z.D. Tomić, A. Kovács, M.D. Joksović, L.S. Jovanović, K. Mészáros Szécsényi. *J. Organomet. Chem.*, **693**, 77 (2008).
[28] B. Holló, V.M. Leovac, P. Bombicz, A. Kovács, L.S. Jovanović, G. Bogdanović, V. Kojić, V. Divjaković, M.D. Joksović, K. Mészáros Szécsényi. *Aust. J. Chem.*, **63**, 1557 (2010).
[29] Oxford Diffraction. *CrysAlis PRO*, Yarnton (2009).
[30] Enraf-Nonius, *CAD-4 Express Software*, Delft, The Netherlands (1994).
[31] A. Altomare, G. Cascarano, C. Giacovazzo, A. Guagliardi, M.C. Burla, G. Polidori, M. Camalli. *J. Appl. Cryst.*, **27**, 435 (1994).

[32] M. Sheldrick. *SHELXL-97, Program for Crystal Structure Refinement*, University of Goettingen, Goettingen (1997).

[33] A.L. Spek. *Acta Cryst.*, **D65**, 148 (2009).

[34] L.J. Farrugia. *J. Appl. Cryst.*, **32**, 837 (1999).

[35] A. Hergold-Brundić, B. Kaitner, B. Kamenar, V.M. Leovac, E.Z. Ivegeš, N. Juranić. *Inorg. Chim. Acta*, **188**, 151 (1991).

[36] V.M. Leovac, Z.D. Tomić, K. Mészáros Szécsényi, Lj.S. Jovanović, M.D. Joksović. *J. Serb. Chem. Soc.*, **72**, 1281 (2007).

[37] Z.D. Tomić, Ž.K. Jaćimović, V.M. Leovac, V.I. Češljević. *Acta Cryst.*, **C56**, 777 (2000).

[38] W.J. Geary. *Coord. Chem. Rev.*, **7**, 81 (1971).

[39] C.F. Macrae, I.J. Bruno, J.A. Chisholm, P.R. Edgington, P. McCabe, E. Pidcock, L. Rodriguez-Monge, R. Taylor, J. van de Streek, P.A. Wood. *J. Appl. Cryst.*, **41**, 466 (2008).

[40] A. Czylkowska, D. Czakis-Sulikowska, A. Kaczmarek, M. Markiewicz. *J. Therm. Anal. Calorim.*, **105**, 331 (2011).

[41] E.B. Okeke, D.V. Soldatov. *J. Therm. Anal. Calorim.*, **100**, 801 (2010).

[42] R. Łyszczek. *J. Therm. Anal. Calorim.*, **108**, 1101 (2012).

[43] R.L. Blaine, H.E. Kissinger. *Thermochim. Acta*, **540**, 1 (2012).

[44] T. Ozawa. *Bull. Chem. Soc. Jpn.*, **38**, 1881 (1965).

[45] G. Singh, C.P. Singh, S.M. Mannan. *Thermochim. Acta*, **437**, 21 (2005).

[46] B.-D. Wu, S.-W. Wang, L. Yang, T.-L. Zhang, J.-G. Zhang, Z.-N. Zhou, K.-B. Yu. *Eur. J. Inorg. Chem.*, **2616**, (2011).

[47] R.D. Gilardi, J. Karle. *The Structural Investigation of Energetic Materials.* In *Chemistry of Energetic Materials*, G.A. Olah, G.R. Squire (Eds.), pp. 2–3, Academic Press, San Diego, CA (1991).